PHILOSOPHICAL MAGAZINE A, 1999, VOL. 79, NO. 3, 655–663

⟨331⟩ slip on {013} planes in molybdenum disilicide

U. V. WAGHMARE†, V. BULATOV ‡, E. KAXIRAS† and M. S. DUESBERY§

† Department of Physics, Harvard University, Cambridge Massachusetts 02138, USA

‡ Department of Mechanical Engineering, Massachusetts, Cambridge, Institute of Technology, Massachusetts 02139, USA

§Fairfax Materials Research, Inc., 7305 Beechwood Drive, Springfield, Virginia 22153, USA

[*Received 13 March 1998 and accepted 29 May 1998*]

ABSTRACT

Branches of the generalized stacking-fault energy surfaces for {013} and {110} planes in molybdenum disilicide are calculated by first-principles density functional methods. The possible antiphase-boundary faults are found to be unstable, but stable stacking faults which permit ⟨331⟩ dislocations to lower their energy by dissociation are found on both planes. Based on the properties of the predicted dissociated dislocations, a qualitative model is advanced to account for the observed features of {013}⟨331⟩ slip in molybdenum disilicide, including the ductile-to-brittle transition.

§1. INTRODUCTION

Molybdenum disilicide ($MoSi_2$) crystallizes in an ordered bct structure with $a = 0.32$ nm and $c = 0.785$ nm, formed by alternate stacking of single Mo and double Si(001) layers, as shown in figure 1 (the larger atoms in figure 1 represent Mo, and the smaller Si). With its high-temperature ductility and exceptional resistance to corrosion and fatigue crack growth, $MoSi_2$ combines the toughness of a metal with the strength of a ceramic and is a promising candidate to replace Ni alloys in the next generation of high-temperature gas turbines. Unfortunately, it undergoes a ductile-to-brittle transition (DBT) at 1200°C, with the fracture toughness dropping to 2–3 MPa $m^{1/2}$. This brittleness at low temperature means that $MoSi_2$ must be formed by costly electrodischarge machining and places a severe limitation on its potential technological utility.

The onset of brittleness is usually due to an increased difficulty in dislocation activity (nucleation or mobility) relative to cleavage. That this may be true for the DBT in $MoSi_2$ is supported by experiment (Gibala *et al.* 1993); pre-straining at 1300°C increases the ductility of polycrystalline $MoSi_2$ at 800°C from zero to 5%, and at 750°C to 1.5%. Further confirmation comes from single-crystal experiments (Ito *et al.* 1995), which show that orientations other than [001] are ductile to room temperature. For [001] orientations, plastic deformation occurs on the {013}⟨331⟩ system, with the flow stress on this slip system increasing rapidly as the DBT temperature is approached from above. This suggests that the onset of brittleness in $MoSi_2$ is due to decreased activity of {013}⟨331⟩ dislocations, leaving no means of accommodation for the component of deformation parallel to the c axis. On the other hand, for orientations close to [100], slip on the {013}⟨331⟩ system is observed for temperatures as low as 0°C (Ito *et al.* 1995), indicating that the

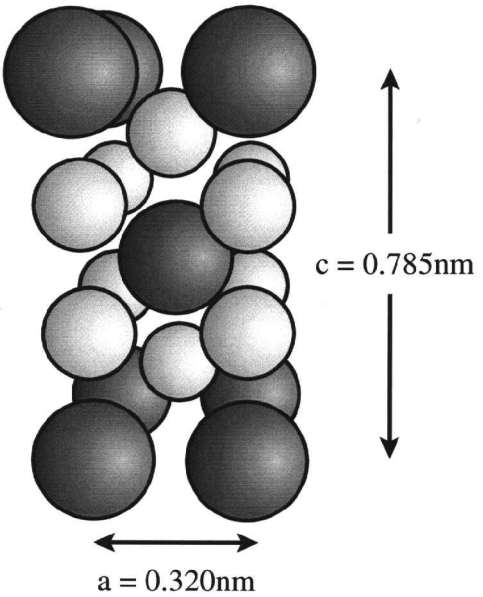

Figure 1. The structure and unit cell dimensions of $MoSi_2$.

governing process for $\{013\}\langle 331\rangle$ slip is strongly orientation dependent (Mitchell and Maloy 1993).

The $\langle 331\rangle$ screw dislocation lies at the intersection of $\{110\}$ and $\{013\}$ planes. This led Umakoshi *et al.* (1990) to suggest that the large high-temperature flow stress is part of a flow stress peak, due to a Kear–Wilsdorf (1962) cross-slip anomaly (Paidar *et al.* 1984) of the type seen in some $L1_2$ compounds. They argued that the phenomenon is driven by a difference in antiphase boundary (APB) energies on $\{110\}$ and $\{013\}$ planes, and deduce from a hard-sphere model that the APB energy is higher on $\{110\}$ than on $\{013\}$ planes. Rao *et al.* (1993), using an embedded-atom model (Daw and Baskes 1983, 1984) approach, concluded that there is no significant difference between the APB energies for the two planes. They suggested that the high flow stress for $\langle 331\rangle$ dislocations is analogous to that observed in bcc metals at low temperatures and is a consequence of the dislocation core structure. TEM observations show that $\{013\}\langle 331\rangle$ dislocations are long and straight (Ito *et al.* 1995), which is indicative of a high Peierls energy and hence of dislocation core effects. The dislocations are of two types, with line direction either $\langle 331\rangle$ (screw character) or $\langle 100\rangle$ (mixed character), with the latter type predominant at high temperatures. Transmission electron microscopy (TEM) indicates (Maloy *et al.* 1993; Ito *et al.* 1995) that the dislocations for both line directions are split into pairs.

In the work reported here, first-principles quantum-mechanical methods are used to calculate parts of the generalized stacking-fault energy γ surface (Vitek 1968) on $\{110\}$ and $\{013\}$, and hence of the possible APBs and stable stacking faults on these planes. It is shown that there are no stable APBs in $MoSi_2$, but that there are stable stacking faults on $\{013\}$ planes. It is argued that the reason for the high flow stress for $\{013\}\langle 331\rangle$ slip in **[001]** crystals is that $\langle 331\rangle$ dislocations are not intrinsic to the $\{013\}$ planes but must be formed by reactions of other dislocations.

§2. Details of calculation

The concept of the γ surface was introduced by Vitek (1968) and can be explained briefly as follows. Consider a crystal cut into two halves parallel to the (*hkl*) plane and suppose that one half is displaced relative to the other by a vector **f**. As this vector is varied to span a unit repeat area in the plane of the cut, the energy $\gamma(\mathbf{f})$ of the crystal changes and traces out the γ surface, which has units of energy per unit area. If the energy is minimized with respect to relative displacement of the crystal halves normal to the fault plane, the fault is referred to as *relaxed*. The power of the γ surface is rooted in its qualitative capability to link microscopic characteristics with macroscopic properties. For example, it can be used at the atomistic level to predict dislocation core properties (Duesbery and Vitek 1998), and also on the macroscopic scale to determine the stress intensity at which dislocations are nucleated at a crack tip (Rice 1992). It is also a fundamental material property which can be calculated from first principles, even for complex materials such as $MoSi_2$. For the purposes of this paper, the usefulness of the γ surface is that, for complex structures, it can determine quantitatively whether or not stable stacking faults can exist.

The γ surface for $MoSi_2$ has been calculated for the [331] direction in the $(0\bar{1}3)$ and $(1\bar{1}0)$ planes, and for the [131] direction in the (013) plane (see figure 2). The first-principles total energy method is based on the local-density approximation (LDA) to density functional theory. A pseudopotential approximation is used to represent ion-electron interaction, with a plane-wave basis to represent electronic wavefunctions and charge density. An optimized pseudopotential for Mo is used (Rappe *et al.* 1990), with semicore s and p levels treated as valence states. Calculations of the lattice constant and bulk modulus of the bulk elemental crystals and $MoSi_2$ show excellent agreement with experiment. An energy cut-off of 60 Ryd has been used to ensure convergence within 1 mRyd atom^{-1}. A Fermi–Dirac broadening scheme with $kT = 0.04$ eV is used to represent the Fermi surface discontinuity and 343 k points are used to sample the Brillouin zone of a single unit cell of $MoSi_2$. The calculation, which has been described in greater detail elsewhere (Waghmare *et al.* 1998), is numerically intensive, particularly in the case of relaxed fault energies. For this reason, relaxation of the faults has been permitted only when its effect is judged likely to affect the inferences drawn from the calculations.

§3. Antiphase boundaries and stacking faults in $MoSi_2$

Projections of the stacking sequence on the $(0\bar{1}3)$ and the $(1\bar{1}0)$ plane are shown in figures 2(*a*) and (*b*) respectively. Only two of the five (013) layers are shown, because the interatomic forces are short ranged. Several prominent crystallographic directions are shown, in particular the [331] vector which is common to both planes. The $\frac{1}{6}[331]$ APB vectors are shown as white arrows superimposed on the black arrows which indicate the $\frac{1}{2}[331]$ Burgers vectors.

The calculated γ surface cross-sections for the $(0\bar{1}3)$ and $(1\bar{1}0)$ planes in the [331] direction are shown in figure 3. The data points are shown as circles $((0\bar{1}3))$ or squares $((1\bar{1}0))$, interpolated by splined curves. The open and full circles represent unrelaxed and relaxed (013) fault energies respectively; none of the $(1\bar{1}0)$ faults was relaxed. There are stable stacking faults, indicated by the metastable energy minima, on both (013) and $(1\bar{1}0)$ planes. To within the accuracy of the calculation, the (013)[331] minima lie at $b/4$ and $3b/4$, where b is the magnitude of the $\frac{1}{2}\langle 331\rangle$ Burgers vector of the perfect dislocation. The corresponding energies are

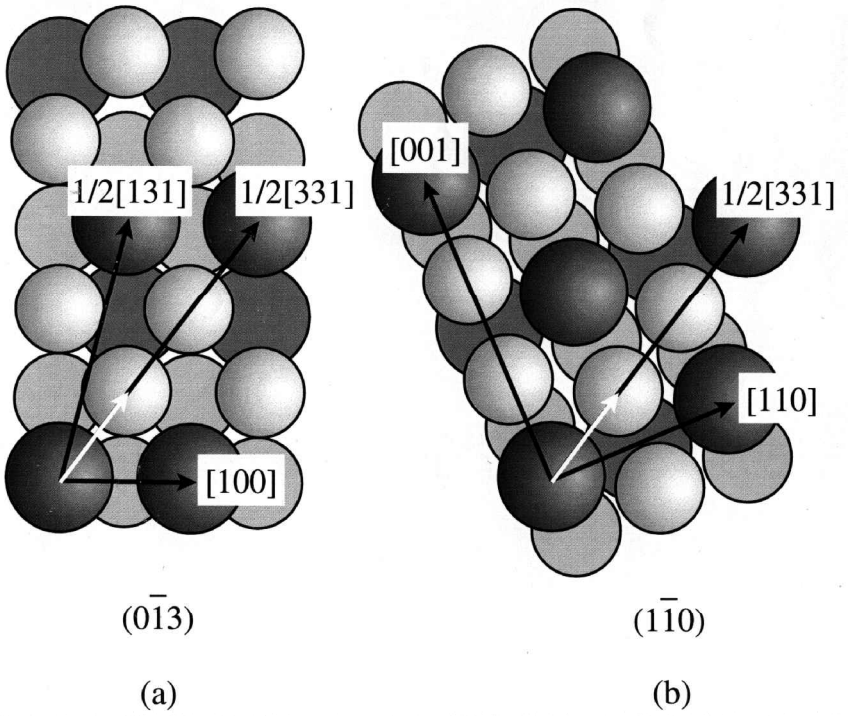

Figure 2. The atomic stacking for (*a*) $(0\bar{1}3)$ and (*b*) $(1\bar{1}0)$ planes in $MoSi_2$.

2.07 J m^{-2} and 1.98 J m^{-2} respectively for the unrelaxed faults. On relaxation, the energies drop to 1.69 J m^{-2} ($b/4$) and 1.86 J m^{-2} ($3b/4$). It is clear that the APB fault $(b/3)$ does not correspond to a local minimum in the γ surface and therefore is unstable. There is similarly no local minimum at the APB location in the $(1\bar{1}0)$ plane (figure 3). However, on this plane there is a pronounced local minimum, with an unrelaxed energy of 0.37 J m^{-2}, lying in the $(1\bar{1}0)[331]$ cross-section at a fault vector of magnitude $b/2$; an extremal value of the γ surface at this point is required by symmetry. Reference to figure 2 (*b*) shows that the lattice stacking produced by this fault (i.e. with a Mo atom sited directly above the midpoint of a line joining two neighbouring silicon atoms) is identical with that produced by the superlattice intrinsic stacking fault (SISF) vector $\frac{1}{4}[111]$. The dislocation dissociation

$$\tfrac{1}{2}[111] \rightarrow \tfrac{1}{4}[111] + \tfrac{1}{4}[111], \qquad (1)$$

in which the partials are separated by a ribbon of SISFs, has been observed by TEM (Evans *et al.* 1993, Ito *et al.* 1995, Maloy *et al.* 1995). Estimates of the energy of the SISF calculated from the partial dislocation separations in equation (1) range from 0.27 to 0.37 J m^{-2} (Ito *et al.* 1995), in good agreement with the LDA calculation. The same fault can also be used as the basis for the $C11_b$ to $C40$ structural transformation in $MoSi_2$ (Inui *et al.* 1998).

The [131] cross-section of the $(0\bar{1}3)$ γ surface has also been calculated for reasons which will become clear in the next section, but is not shown. There is a stable stacking fault at a vector of 0.3[131], with an unrelaxed energy of 2.40 J m^{-2}. The

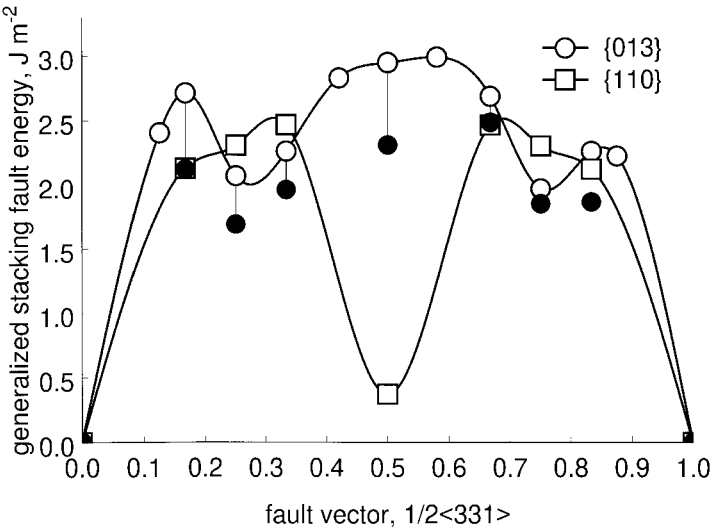

Figure 3. The ⟨331⟩ branch of the generalized stacking-fault energy surface for {013} and {110} planes in $MoSi_2$.

relaxed energy for this fault has not been calculated; based on the ⟨331⟩ results, it could be up to 20% lower than the unrelaxed energy.

The results of this calculation demonstrate clearly that the hard-sphere and the central-force models can be deceptive when dealing with complicated materials in which there is strongly directional (covalent) bonding.

§4. Dislocation dissociation in $MoSi_2$

The occurrence of $\{013\}\langle 331\rangle$ slip is unexpected for geometric reasons. This particular slip system is unusual in that, of all repeat vectors in the $(0\bar{1}3)$ plane with a component in the direction of the c axis (figure 2), the $\frac{1}{2}\langle 331\rangle$ Burgers vector is not the smallest (it can be noted that the smallest repeat vector in this plane is [100], but this has no c component and is therefore excluded from consideration). On the basis of the Frank (1949) criterion, in which the energy of a dislocation is taken to be proportional to the square of the Burgers vector, the $\frac{1}{2}[131]$ dislocation, with $b = 0.64$ nm, is strongly preferred over the observed $\frac{1}{2}[331]$ dislocation, which has $b = 0.78$ nm. The existence of metastable minima in the γ-surface cross-sections, however, means that the dislocations can dissociate into partial dislocations separated by stable stacking faults. Based on the γ surface cross-sections of the previous section, the possible reactions are given by

$$\begin{aligned} \tfrac{1}{2}[131] &\rightarrow \tfrac{1}{5}[131] + \tfrac{3}{10}[131], \\ \tfrac{1}{2}[331] &\rightarrow \tfrac{1}{8}[331] + \tfrac{1}{4}[331] + \tfrac{1}{8}[331], \end{aligned} \tag{2}$$

on the $(0\bar{1}3)$ plane and

$$\tfrac{1}{2}[331] \rightarrow \tfrac{1}{4}[331] + \tfrac{1}{4}[331] \tag{3}$$

on $(1\bar{1}0)$. The second dissociation in equation (2), with all three partials assumed to be of equal magnitude, has been observed (Boldt *et al.* 1992) around indentations.

If the Frank criterion is applied to the reaction products in equation (2), as is often done, the dissociated dislocations would be judged equal in energy to a few per cent. However, this would be incorrect. The Frank criterion neglects elastic anisotropy and, when applied to dissociated dislocations, neglects the elastic interactions and the energy of the stacking faults. For the present purposes, the energy of a dislocation which has a total Burgers vector b_T and which is dissociated into partials with Burgers vectors b_i and positions r_i can be written as

$$E = \frac{K}{4\pi}\sum_i b_i^2 \ln\left(\frac{R}{b_T}\right) + \frac{K}{2\pi}\sum_i \sum_{j>i} b_i b_j \ln\left(\frac{R}{|r_i - r_j|}\right) + \sum_i \gamma(|r_{i+1} - r_i| - b_T)$$

$$= \frac{K}{4\pi} b_T^2 \ln\left(\frac{R}{b_T}\right) - \frac{K}{2\pi}\sum_i \sum_{j>1} b_i b_j \ln\left(\frac{|r_i - r_j|}{b_T}\right) + \sum_i \gamma(|r_{i+1} - r_i| - b_T), \qquad (4)$$

where K is the appropriate anisotropic elastic energy factor. R is the screening length for the dislocation distribution in the bulk solid (a value of 1 μm has been used). The terms on the right-hand side of the second equation in equation (4) correspond, in order, to the self energy E_S of the perfect dislocations, the interaction energy and the stacking fault energy. The energy within a core cylinder of radius b_T has been excluded from each term.

Table 1 shows the energies computed from equation (4) for the three dissociation models in equations (2) and (3) applied to screw dislocations. For each case the table lists the separation of the partials, the dimensionless stacking-fault energy $4\pi\gamma/Kb_T$, the self-energy E_S and the total energy E from equation (4). Since $|r_i - r_j| \ll R$ and $4\pi\gamma/Kb_T \ll \ln(R/b_T)$, it is clear that the dominant term is the self-energy (i.e. the Frank energy for the perfect dislocation). For example, the dissociations (2) do little to modify the conclusion, based on the Frank criterion, that the energy of $\frac{1}{2}\langle 311\rangle$ dislocation is about 50% larger than that of the $\frac{1}{2}\langle 131\rangle$ dislocation. For the third dissociation (3), which involves the low-energy SISF, the Frank energy is still the dominant term, but the effect of the much wider dissociation is to reduce the energy of the $\frac{1}{2}[331]$ dislocation by 14% (see table 1).

The linear elastic energy (4) is an approximation for several reasons, which will not be discussed in detail here (see Duesbery (1998) for a treatment of nonlinear effects in dislocation dissociation in copper). It is sufficient for the present purposes to note that the self energy E_S (first term 1 in equation (4)) is a reliable estimate of the elastic energy of the perfect dislocation. The remaining terms in equation (4) are also expected to be a good estimate of the interaction and stacking-fault energies of a

Table 1. Dislocation dissociation energies for selected $\frac{1}{2}[131]$ and $\frac{1}{2}[331]$ dislocations on $(0\bar{1}3)$ and (110). E_S is the self-energy of the perfect dislocation and E is the energy of the dissociated dislocation. Note that $1\,\mathrm{nJ\,m^{-1}} = 0.63\,\mathrm{eV\,\AA^{-1}}$.

Plane and Burgers vector	Line	r nm	$4\pi\gamma/Kb_T$	E_S ($\mathrm{nJ\,m^{-1}}$)	E ($\mathrm{nJ\,m^{-1}}$)
$(0\bar{1}3)\frac{1}{2}[131]$	[131]	1.48	0.202	44.8	44.0
$(0\bar{1}3)\frac{1}{2}[331]$	[331]	1.44	0.174	63.5	61.9
$(1\bar{1}0)\frac{1}{2}[331]$	[331]	14.90	0.026	63.5	54.6
$(1\bar{1}0)\frac{1}{2}[111] + (001)[110]$	[100]	14.90		75.6	39.5

dissociated dislocation, provided that the partials are well separated, as in the dissociation (3). For small separations, such as those in the dissociations (2), the interaction and stacking-fault energies given by equation (4) will not be as accurate, but in this case these terms amount only to a small perturbation of the self-energy, and therefore the total energy is still expected to be reliable.

Since the energy of the $\frac{1}{2}[131]$ dislocation is very much lower than that of the $\frac{1}{2}[331]$ dislocation, any grown-in dislocations on $(0\bar{1}3)$ planes are expected to be of the former type. It is therefore suggested that the observed ⟨331⟩ dislocations are not intrinsic to {013} planes but have another origin. A suitable source for the $\frac{1}{2}[331]$ screw dislocation is the dissociation (3). In this model, ⟨331⟩ screw dislocations can exist in low-energy dissociated form on {110} planes. The two partials in the model and their separation of about 15 nm are consistent with TEM observations (Ito *et al.* 1995).

The second prominent line direction observed for $\frac{1}{2}[331]$ dislocations is **[100]**. The dislocation image is split in this case also, but the Burgers vectors of the product dislocations have not been established unequivocally. It has been suggested that the dissociation is not into partial dislocations, but into perfect dislocations with smaller Burgers vectors, after the reaction (Mitchell *et al.* 1992):

$$\tfrac{1}{2}[331] \rightarrow \tfrac{1}{2}[111] + [110]. \qquad (5)$$

TEM observations are consistent with equation (5) (Ito *et al.* 1995). The product dislocations in equation (5) are not glissile on $(0\bar{1}3)$. In order to share the **[100]** line direction and to be able to glide apart, the $\frac{1}{2}[111]$ and **[110]** dislocations must move on $(0\bar{1}1)$ and (001) respectively. The energy change in this reaction is included in table 1. In this case the self-energy E_S is that of a $\frac{1}{2}[331]$ dislocation with **[100]** line direction lying on the $(0\bar{1}3)$ plane. The energy E of the dissociated complex is the sum of the self-energies of the product dislocations and their interaction energy at an arbitrarily chosen separation of 14.9 nm, the same as for the screw dissociation (3).

§5. Discussion and conclusions

It has been shown, using first-principles calculations, that there are stable stacking faults in $MoSi_2$ for fault vectors in the ⟨331⟩ direction on both {013} and {110} planes, and in the ⟨131⟩ direction on {013} planes. The stacking fault with the lowest energy occurs for a fault vector $\frac{1}{4}\langle 331\rangle$ on {110} and is identical with the $\frac{1}{4}\langle 111\rangle$ SISF. The calculated energy for this fault is $0.37\ \mathrm{J\,m^{-2}}$, in good agreement with the range of values of 0.17–$0.37\ \mathrm{J\,m^{-2}}$ estimated from experiment (Ito *et al.* 1995).

Although they do not correspond to APB faults, the stable stacking faults permit dislocation dissociation into pure screw partials and are geometrically compatible with the Kear–Wilsdorf hardening proposed by Umakoshi *et al.* (1990). However, this hypothesis requires that the fault energy be lower on {013}. Calculation indicates that the {013} faults have an energy about five times that of the {110} fault, and therefore the proposed cross-slip anomaly is unlikely.

The alternative suggestion, that a dislocation core mechanism is responsible (Rao *et al.*1993), is considered more reasonable. Dislocations with $\frac{1}{2}\langle 131\rangle$ Burgers vector are not observed on {013} planes, despite their much lower energy than dislocations with the $\frac{1}{2}\langle 331\rangle$ Burgers vector. This is an indication that $\frac{1}{2}\langle 331\rangle$ dislocations are not native to the {013} plane. It is suggested that the ground state for $\frac{1}{3}\langle 331\rangle$ dislocations is the dissociation (3) into two $\frac{1}{4}\langle 331\rangle$ partials separated by a low-energy SISF. In order to slip on {013}, dissociated screw dislocations must cross-slip from {110}.

This requires the creation of a high-energy fault on {013} (see equation (2)) and will be a thermally activated process. Once transferred to {013}, the $\frac{1}{2}\langle 331\rangle$ screw dislocations can move and trail arms of mixed dislocation with line direction $\langle 100\rangle$. These mixed dislocations can dissociate into a ground state consisting of two smaller perfect dislocations after equation (5), resulting in a large decrease in energy. The product dislocations cannot glide on or cross-slip to {013} and therefore must be constricted together before motion on {013} can occur. The energy which must be supplied to reverse the reaction (5) is four times that required for reaction (3). The mixed dislocation arms will have a much lower mobility than the screw dislocations and the latter will be primarily responsible for $\langle 331\rangle\{013\}$ plasticity. Because the constituent dislocations in the ground states lie on different planes and have different Burgers vectors, the dislocation mobility is expected to be strongly orientation dependent.

Two cases will now be considered. The first case is for stress orientations other than [001]. There will be stress components acting to assist the recombination of both of the $\frac{1}{2}\langle 331\rangle$ dislocation ground states. At low temperatures, when the mobilities of both types of dislocation are very low, similar numbers of screw and mixed dislocations are expected. At high temperatures the mobility of screw dislocations will increase more rapidly than that of the mixed dislocations, because of the lower activation energy. It is then expected that the density of mixed dislocations will be much higher than that of screw dislocations. This qualitative result is in agreement with experiment (Ito *et al.* 1995). When the applied stress acts along [001], there is no resolved stress on the {110} plane acting to constrict the dissociated screw dislocation, and therefore the mobility will drop sharply, introducing a DBT at the temperature for which crack propagation becomes thermodynamically preferred. There is a resolved stress on one ($\frac{1}{2}\langle 111\rangle\{011\}$) of the mixed dislocation constituents, but the mobility of this dislocation is so low that this will not make a significant difference.

The dislocation ground states predicted above are based on quantitative first-principles calculations and agree with experimental observations. The mobility arguments which are developed from these dislocation structures are qualitative and less firmly based but are also compatible with experimental results. There is a clear need for atomistic calculations, to confirm the dislocation ground states and to determine the mechanisms of and energies required for activation into mobile states, and for mesoscale models to evaluate the kinetics of plastic flow in $MoSi_2$.

Acknowledgement

This work was performed with support from the Office of Naval Research under N00014-97-C-0104.

References

Boldt, P. H., Embury, J. D., and Weatherly, G. C., 1992, *Mater. Sci. Engng.,* **A155**, 251.

Daw, M. S., and Baskes, M. I., 1983, *Phys. Rev. Letters,* **50**, 1285; 1984, *Phys. Rev.* B, **29**, 6443.

Duesbery, M. S., 1998, *Modelling Simulation Mater. Sci. Engng.,* **6**, 35.

Duesbery, M. S., and Vitek, V., 1998, *Acta Mater.,* **46**, 1481.

Evans, D. J., Court, S. A., Hazzledine, P. M., and Fraser, H. L., 1993, *Phil. Mag. Lett.,* **67**, 331.

Frank, F. C., 1949, *Physica,* **15**, 131.

Gibala, R., Chang, H., and Czarnik, C. M., 1993, *High Temperature Silicides and Refractory Alloys,* Materials Research Society Symposium Proceedings, Vol 322 (Pittsburgh, Pennsylvania: Materials Research Society), p. 49.

Inui, H., Moriwaki, M., Ito, K., and Yamaguchi, M., 1998 (to be published).

Ito, K., Inui, H., Shirai, Y., and Yamaguchi, M., 1995, *Phil. Mag.* A, **72**, 1075.

Kear, B. H., and Wilsdorf, H. G. F., 1962, *Trans AIME,* **224**, 382.

Maloy, S. A., Mitchell, T. E., and Heuer, A. H., 1995, *Acta metall. mater.,* **43**, 657.

Maloy, S. A., Mitchell, T. E., Lewandowski, J. J., and Heuer, A. H., 1993, *Phil. Mag. Lett.,* **67**, 313.

Mitchell, T. E., Castro, R. G., and Chadwick, M. M., 1992, *Phil. Mag.* A, **65**, 1339.

Mitchell, T. E., and Maloy, S. A., 1993, *Critical Issues in the Development of High Structural Materials* (Warrendale, Pennsylvania: Metallurgical Society of AIME).

Paidar, V., Pope, D. P., and Vitek, V., 1984, *Acta metall.,* **32**, 435.

Rao, S. I., Dimiduk, D. M., and Mendiratta, M. G., 1993, *Phil. Mag.* A, **68**, 1295.

Rappe, A. M., Rabe, K. M., Kaxiras, E., and Joannopoulos, J. D., 1990, *Phys. Rev.* B, **41**, 1227.

Rice, J. R., 1992, *J. Mech. Phys. Solids,* **40**, 239.

Umakoshi, Y., Sakagami, T., Hirano, T., and Yamane, T., 1990, *Acta. metall. mater.,* **38**, 909.

Vitek, V., 1968, *Phil. Mag.,* **18**, 773.

Vaghmare, U. V., Bulatov, V., Kaxiras, E., and Duesbery, M. S., 1998, *Modelling Simulation Mater. Sci. Engng* (in the press).